

5.3 Scientific Achievements

5.3.1 Building blocks of dynamical heterogeneities in dense granular media

Glassy materials and granular media are two "states" of matter that share properties with both the liquid and solid ones. Under different conditions they can flow like liquids or behave like solids. In particular granular materials get "jammed" at high density while the flow of glasses is dramatically slowed down at low temperature. It has been suggested that both transitions are governed by similar underlying physical mechanisms. One of the recent advances in these fields has been the introduction of dynamical heterogeneities. The aim of this work was to characterize these DH in a system where the trajectory of each grain can be determined.

The experimental setup consisted in a monolayer of bidisperse cylinders at a high volume fraction and periodically sheared. The position of each grain is followed by taking images of a large field: this allows the computation of four point correlation functions, which are the ideal tools to capture "amorphous order", whether it be dynamical or static. Due to the trapping of any given particles by its neighbors, we find that the individual trajectories of the grains are subdiffusive at short times. They become diffusive only at times larger than the "cage jump time". We have designed a special algorithm allowing to detect very accurately all the cage jumps events and found that the cage jump time τ^* is close to 700 cycles in our setup. Figure 31 displays a sample trajectory showing a diffusive motion between successive cage jumps.

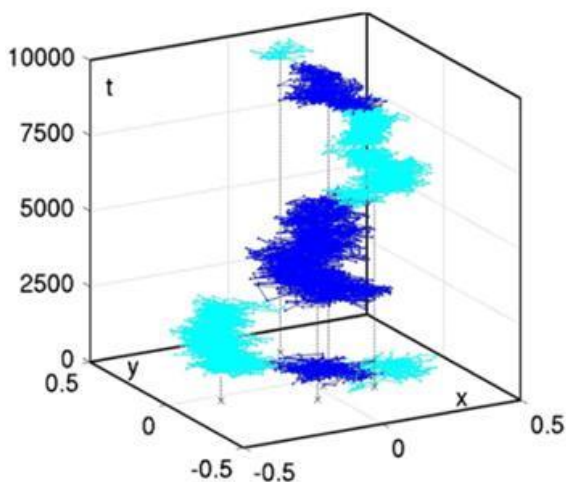


Figure 31 3D visualization of the trajectory of a single particle. The color changes each time the algorithm detects a cage jumps. Distances are scaled to the radius of grains and $t=1$ is the duration of a mechanical cycle.

A global overview of these jumps reveals the important information that these jumps are correlated in time and space. Indeed, as shown in Figure 32 (left) they occur in short bursts (about 10 cycles long) involving groups of neighboring particles. The size distribution of these groups is however

widely distributed. It can be fitted with a power law distribution with exponent between 1.5 and 2 (Figure 32, right).

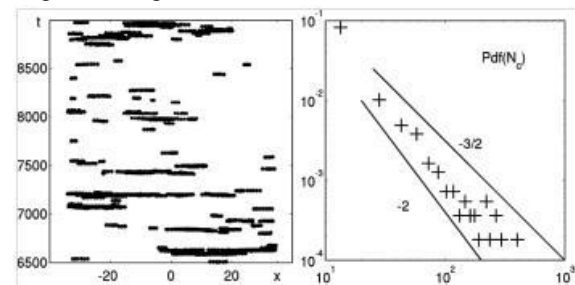


Figure 32 Left: Spatiotemporal position of the cage jumps: only one direction in space is shown (x axis). Each point represents a cage jump. The very flat clouds of points are clusters of collective and instantaneous cage jumps. Right: Probability distribution of cluster sizes.

On longer time scales one can show that these bursts are not all independent. Indeed the distribution of durations between two successive bursts does not show a Poissonian distribution but two different regimes, which can be explained by considering that each "original" burst triggers echoing ones. A detailed analysis shows that the bursts of cage jumps aggregate temporally and spatially in "avalanches" to build ultimately the large scales dynamical heterogeneities.

This non local space and time character might be a key in matching theoretical models. For example, we have shown that the so called "dynamic facilitation", put forward in some models, clearly plays a role in the development of the avalanche process, but that it is irrelevant to trigger it. More generally, this study opens the way to a better understanding of the glassy state and of the glass transition.⁶⁹

⁶⁹R. Candelier, O. Dauchot and G. Biroli, *Phys. Rev. Lett.* **102** (2009) 088001.

5.3.2 Increase of the dynamical correlation volume during aging of glycerol

When a supercooled liquid is quenched below its glass transition temperature T_g , its properties age, i.e. they depend on the time t_a elapsed since T_g was crossed. By recording the nonlinear response $\chi_3(t_a)$, we show that the dynamical correlation volume increases with t_a . This first of the kind experiment allows for a better microscopic understanding of the glassy state and shows on which spatio-temporal scale a glass moves from solid to liquid behavior.

Understanding what happens at the glass transition still remains a challenge. On the one hand the temperature dependence of the viscosity η is faster than an Arrhenius law, which suggests that there exists a correlation volume which grows when decreasing the temperature T . On the other hand there is no sign of structural correlations in, e.g. the neutron diffusion spectra. To solve this conundrum, the glass community has built the so-called dynamical heterogeneity scenario where the correlations are to be found in the movements of the particles: the relaxation time τ_α does not come from single molecule displacements, but from the collective motion of N_{corr} particles, some groups being faster than others - hence the name of Dynamical Heterogeneities (DH) for these groups. According to some theories, the increase of N_{corr} when T decreases towards T_g would be the reason for the super-Arrhenian behavior of η . Moreover N_{corr} was predicted to be proportional to the nonlinear susceptibility χ_3 . Our pioneering dielectric measurements of χ_3 have been found to be consistent with this scenario, at least at equilibrium, i.e. above T_g .⁷⁰

We have pushed our χ_3 measurements into the aging regime where the properties depend on the age t_a elapsed since T_g was crossed. During aging the evolution of χ_3 stems both from the increase of τ_α (stiffening) and from that of N_{corr} . To disentangle these two effects, stiffening was independently obtained from the aging of the linear susceptibility χ_{lin} - where χ_{lin} is independent of N_{corr} -. This is how we obtain the results summarized in Figure 33 where it is shown that, at $0.96T_g$, N_{corr} increases with t_a before reaching its equilibrium value after 100 ks. This first of the kind result for the aging of N_{corr} has several important consequences.⁷¹ It shows that below T_g , a glass behaves as a liquid. The $N_{\text{corr}}(t_a)$ behavior -colored points- is indeed very close to what is obtained by extrapolating the $N_{\text{corr}}(T)$ dependence obtained at equilibrium above

T_g and by using the fictive temperature (black line). This conclusion about the liquid behavior of the glass below T_g is reinforced by the fact that aging eventually stops and yields a finite value for N_{corr} . This liquid state below T_g is however very peculiar since it contains highly non trivial correlations where the relaxation events happen through domains gathering N_{corr} particles. This is the “solid” aspect of the glasses below T_g .

Besides, by gathering our equilibrium and non equilibrium χ_3 experiments, the number of decades of τ_α is large enough to test various theories aiming at describing the glassy state. The inset of Figure 33 shows that two of them are found to be consistent with our data. At least one other theory is contradicted by our data. This shows that our nonlinear susceptibility experiments are able to really test some of the theories of the glass transition.

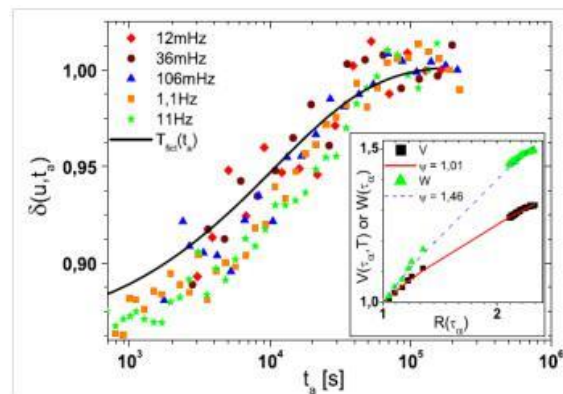


Figure 33 Behavior of $\delta = N_{\text{corr}}(t_a) / N_{\text{corr}}(\text{eq})$ as a function of the age t_a in glycerol at $0.96T_g$. Inset: test of two theories predicting the evolution of the number N_{corr} of dynamical correlated particles.

⁷⁰C. Crauste-Thibierge, C. Brun, F. Ladieu, D. L'Hôte, G. Biroli, J.-P. Bouchaud, *Phys. Rev. Lett.* **104** (2010) 165703.

C. Brun, F. Ladieu, D. L'Hôte, M. Tarzia, G. Biroli, J.-P. Bouchaud, *Phys. Rev. B* **84** (2011) 104204.

⁷¹C. Brun, F. Ladieu, D. L'Hôte, G. Biroli, J.-P. Bouchaud, *Phys. Rev. Lett.* **109** (2012) 175702.

5.3.3 Violation of Fluctuation-Dissipation-Theorem in Superspin Glass

The fluctuation-dissipation theorem (FDT) relates the intensity of thermal fluctuations of an observable (noise) to the response to a perturbation (susceptibility). It is a principle verified in all systems at thermodynamic equilibrium. We have examined the validity of the FDT in a frozen ferrofluid and showed that FDT is violated in the low temperature superspin glass phase.

The fluctuation-dissipation theorem (FDT) states that in a given system in thermal equilibrium, the linear response to an external perturbation can be expressed in terms of its fluctuation. In its simplest form, FDT is described as:

$$S_x(\omega) = \frac{2k_B T}{\omega} \text{Im} \hat{\chi}(\omega)$$

Where $S_x(\omega)$ is the power spectrum (noise) of the observable x as a function of frequency ω and $\text{Im} \hat{\chi}(\omega)$ is the imaginary part of the susceptibility $\chi(\omega)$. It is one of the most notable achievements of statistical thermodynamics and has been proven in a plethora of real physical systems; *e.g.* the thermal noise in a resistor and the Brownian motion of particles in a fluid. However, equilibrium behavior is the exception rather than the rule in Nature. The evolution of most physical systems involves transport of mass, energy, charge, etc., not compatible with equilibrium where the FDT applies. To this end, many experimental and theoretical attempts have been made to extend the FDT to out-of-equilibrium for the last three decades.⁷² According to certain models, the FDT may be adapted in out-of-equilibrium state, by replacing the temperature T by the effective temperature T_{eff} . The ratio T_{eff}/T indicates the degree of “out-of-equilibrium’ness” of the system. The larger the deviation from unity of this value, the further from equilibrium the system is.

Glasses are naturally out-of-equilibrium systems made of disordered interacting elementary components. They include not only standard glasses (vitreous silica), but also molecular and metallic glasses, polymers, colloids, ceramics, gels, granular systems and even electron and spin (magnetic) glasses. One of the main characteristic of glasses is that their relaxation times exceed common time-scales, thus they never reach equilibrium; making them an ideal candidate to test if and how the FDT is violated. The study of FDT violation has so far been carried out on diverse glasses, yet very few experimental evidences exist due to the difficulty of measuring small “noise” signals. With researchers in LSI/IRAMIS, we have tested the FDT on a special type of magnetic glass; namely Superspin glass

made out of interacting magnetic nanoparticles ($\gamma\text{-Fe}_2\text{O}_3$) suspended in a frozen liquid matrix (ferrofluid). Nanoparticles are single-domained and carry huge magnetic moments of $\sim 10^4 \mu\text{B}$, thus called “superspins.” When the system is cooled below the transition temperature T_g , the superspins become progressively correlated to one another due to dipolar interactions, forming a glassy, slowly evolving collective state.

To test the FDT, we have measured the noise in local magnetic field induced by the sample’s magnetization fluctuation in its superspin glass state, $S_x(\omega)$, using a micro-Hall sensor ($2 \times 2 \mu\text{m}^2$). A small quantity of ferrofluid (7 picoliter) is deposited directly onto the sensor surface (Figure 34). The noise spectra were then compared to the frequency dependent magnetic susceptibility, $\chi(\omega)$, measured using a SQUID magnetometer.

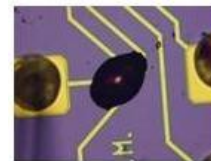


Figure 34 A small drop of ferrofluid deposited on the micro-Hall sensor surface.

At high temperature, $T > T_g$ ($=67 \text{ K}$), the ratio between the effective and measured temperatures T_{eff}/T is indeed equal to unity as expected from the FDT. But the ratio deviates from unity quickly at low temperature, indicating the violation of the FDT in the superspin glass phase (Figure 2). Our observation is the first experimental evidence of the FDT violation in a superspin glass, and only a second of its kind in magnetic spin-glass systems.⁷³

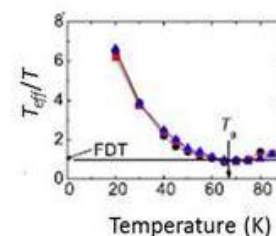


Figure 35 T_{eff}/T at various frequencies as a function of temperature.

⁷²L.F. Cugliandolo and J. Kurchan, *J. Phys. A* **27** (1994) 5749.

⁷³K. Komatsu, D. L’Hôte, S. Nakamae, V. Mosser, M. Konczykowski, E. Dubois, V. Dupuis and R. Perzynski, *Phys. Rev. Lett.* **106** (2011) 150603.

5.3.4 Von Kármán sodium dynamo

Flows of electrical conducting fluids interact with electromagnetic fields, allowing conversion between mechanical and electromagnetical energy. These energy transfers are involved in a wide range of phenomena from astrophysical and geophysical flows, where conducting fluid flows generate magnetic fields by dynamo action, to industrial processes, where magnetic fields and currents are used to move and stir liquid metals. We present in the following new instabilities obtained in MHD driven flows and the breakthrough realized in the VKS experiment.

Electromagnetic fields are sensitive to liquid metal flows through distortion and advection of the field lines induced by the induction equation. Conversely, currents and magnetic fields act on liquid metals via the Lorentz Force that has to be introduced in the Navier-Stokes equation. Hence, instabilities transferring electromagnetic energy to mechanical energy are possible and used for Linear Electro-Magnetic Pump with Annular Induction (ALIP) which are planned to be used at high flow rates in the secondary cooling circuits of the fourth generation Nuclear Reactor. Once the fluid is moved, it is crucial to insure a constant flow rate and hence to inhibit all instabilities that could reduce the cooling efficiency. In an electromagnetically driven model flow, we have exhibited two new wave instabilities, with different response to the applied magnetic field.⁷⁴

When a liquid metal is strongly stirred by an external mechanical or thermal forcing, a magnetic field can be generated by dynamo instability. This mechanism is invoked to explain most of the magnetic fields of the astrophysical objects. Due to the extremely low value of the ratio of the viscous diffusivity over the magnetic diffusivity, a great amount of mechanical energy is necessary to exceed the –unpredictable– dynamo onset, leading to very large turbulent fluctuations, except for highly constrained flows (Riga and Karlsruhe dynamo experiments). The von Karman Sodium (VKS) experiment based in CEA Cadarache in collaboration with CNRS, ENS and ENS-Lyon, was the first to reach the dynamo onset in an unconstrained turbulent flow. Moreover, the flow, generated between two iron impellers in a cylindrical vessel, is able to generate various dynamical behaviors of the dynamo magnetic field depending on the relative velocity of the impellers: constant (although fluctuating) dipolar structure appearing for exact counter-rotating case, periodic or erratic inversions of the magnetic fields, temporary extinction etc.,⁷⁵ when the relative velocity of the impeller is shifted.

Most of these regimes can be captured within a minimal dynamical model based on the symmetries of the system, involving only two magnetic modes and a noise mimicking the turbulent fluctuations. Among the model achievements are the prediction of bistability,⁷⁶ and the localization of the magnetic field in half of the cell, which have been observed in the experiment.⁷⁷ In parallel, reconstruction methods have been developed, in order to confirm all the spatial structure of magnetic field, probed by a limited numbers of local sensors.⁷⁸

Most of the observed regimes have astrophysical and geophysical relevance: erratic inversions shared strong similitude with the Earth's magnetic field dynamics, periodic regimes recall the 22 year period of sunspot activity and the fossil magnetic field of Mars keeps track of its localization in one hemisphere. Despite all these successes, the VKS dynamo is not still an ended story. Indeed, although the dynamic of the magnetic field is now well understood, the mechanism of the magnetic field generation is still puzzling. Indeed, despite numerous experimental tests, none of the proposed models satisfactory explains the primordial roles of the full iron impellers which are absolutely necessary to observe dynamo within the parameter range available in the VKS experiment.⁷⁹

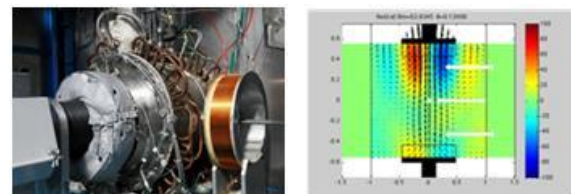


Figure 36 Left: Picture of the van Karman Sodium experiment. Right: Snapshot of the magnetic field localized in near one disk. The magnetic field has been reconstructed from 40 discret sensors located in the four probes materialized by the white stripes. Arrows show the poloidal part of the field, colors encode the intensity of the toroidal part.

⁷⁴J. Boisson *et al.*, *Phys. Fluids* **24** (2012) 044101.

⁷⁵R. Monchaux *et al.*, *Phys. Fluids* **21** (2009) 035108.

⁷⁶M. Berhanu *et al.*, *JFM* **641** (2009) 217-226.

⁷⁷B. Gallet *et al.*, *Phys. Rev. Lett.* **108** (2012) 144501.

⁷⁸J. Boisson and B. Dubrulle, *New J. Phys.* **13** (2010) 023037; J. Boisson *et al.*, *New J. Phys.* **14** (2012) 013044.

⁷⁹F. Ravelet *et al.*, *Phys. Rev. Lett.* **109** (2012) 024503.

5.3.5 Unveiling a phase transition in turbulence.

We experimentally study the response to symmetry breaking of a closed turbulent von Kármán swirling flow from $Re=150$ to $Re=10^6$. Depending on the forcing, we report a subcritical or a continuous transition associated to a divergence of the susceptibility at an intermediate Reynolds number ($Re=40\,000$). These results provide experimental evidence that such a highly space and time fluctuating out-of-equilibrium system can undergo a “phase transition”.

Phase transitions are ubiquitous in physical systems and generally associated with symmetry breaking. For example, ferromagnetic systems are well known to undergo a phase transition from paramagnetism to ferromagnetism at the Curie temperature T_c . This transition is associated with a symmetry breaking from the disordered paramagnetic—associated with a zero magnetization—toward the ordered ferromagnetic phase—associated with a finite magnetization. In the context of fluid dynamics, symmetry breaking also governs the transition to turbulence that usually proceeds, as the Reynolds number Re increases, through a sequence of bifurcations breaking successively the various symmetries allowed by the Navier-Stokes equations coupled to the boundary conditions. Finally, at large Reynolds number, when the fully developed turbulent regime is reached, it is commonly admitted that all the broken symmetries are restored in a statistical sense, the statistical properties of the flow not depending anymore on Re . However, both natural systems and recent experimental studies of turbulent flows have shown the possible existence of turbulent transitions between some “mean states”. Consequently, despite the fact that turbulent flows are intrinsically out-of-equilibrium systems, one may wonder whether the observed transitions can be interpreted in terms of phase transitions.

Using the von Karman flow as a model turbulent experiment, we have studied the subcritical or supercritical response of the turbulent flow to a continuous breaking of its forcing symmetry from $Re=150$ to $Re=10^6$. In the first case, the mean flow presents multiple solutions, the bifurcation between these states is highly subcritical and the system keeps a memory of its history. The transition recalls low-dimension dynamical system transitions and exhibits very peculiar statistics. We have further studied the influence of the stability of such steady states under two different forcing conditions, either imposing the speed or the torque to our impellers. We found that the different forcing conditions change the nature of the stability of the steady states and reveal dynamical regimes that bear similarities with low-dimensional systems. We can consider our forcings to be conjugate, as the product torque

X speed controls the energy injection rate in our experiment. Switching from speed to torque control might then be seen as an analogue of switching from canonical to microcanonical ensemble. We thus suggest that the forcing dependence we found may be an out-of-equilibrium analogue of the ensemble inequivalence, valid for long-range interacting statistical systems, and that it may be applicable to other turbulent systems.⁸⁰

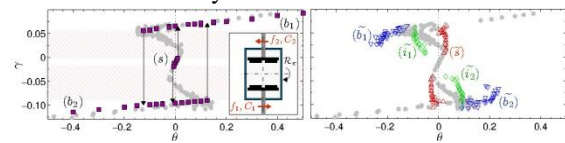


Figure 37 Mean Torque vs. mean velocity difference under two forcing conditions: left: constant speed applied to impellers; right: constant torque applied to impellers. Note the new “i” states appearing in the second case.

In the second case, we report a divergence of the susceptibility to symmetry breaking at a critical Reynolds number $Re=40\,000$ revealing a phase transition, analogous to the para-ferromagnetic transition. This transition is furthermore associated with a change in the statistical properties and a peak in the amplitude of fluctuations of the instantaneous flow symmetry corresponding to intermitencies between spontaneously symmetry breaking metastable states.⁸¹

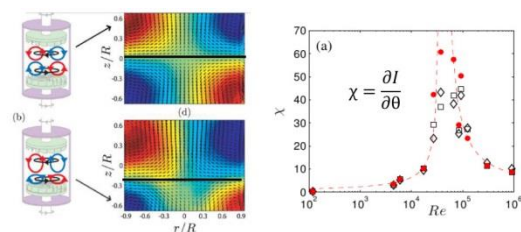


Figure 38 Left: Sketch of the symmetry of the experiment, and view of the spontaneous symmetry breaking states. Right: susceptibility to symmetry breaking as a function of the Reynolds number. Note the divergence occurring around $Re=40000$.

⁸⁰P.-P. Cortet *et al.*, *Phys. Rev. Lett.* **105** (2010) 214501; P.-P. Cortet *et al.*, *J. Stat. Mech.* (2011) P07012.

⁸¹B. Saint-Michel *et al.*, submitted to *Phys. Rev. Lett.*

5.3.6 Climate

The Earth, like other planets with a relatively thick atmosphere, is not locally in radiative equilibrium and the transport of energy by the geophysical fluids (atmosphere and ocean) plays a fundamental role in determining its climate. Using simple energy-balance models, it was suggested a few decades ago that the meridional energy fluxes might follow a thermodynamic Maximum Entropy Production (MEP) principle. In the present study, we assess the MEP hypothesis in the framework of a minimal climate model based solely on a robust radiative scheme and the MEP principle, with no extra assumptions. The climate model presented here is extremely fast, needs very little empirical data and does not rely on ad hoc parameterizations. We investigate its range of validity by comparing its performances for pre-industrial climate and Last Glacial Maximum climate with corresponding simulations with the IPSL coupled atmosphere-ocean General Circulation Model IPSL_CM4, finding reasonable agreement.

The Earth receives a certain amount of energy from the Sun, in the form of visible light, which it has to radiate back to space, in the form of infrared light, to maintain a steady state. Most Earth System processes, including weather and climate, can be regarded as little more than steps in this process of energy conversion from one form to the other, going through various other forms of energy (potential energy, kinetic energy, heat...). In each of these steps the overall quantity of energy has to be conserved. Modeling this energy exchange is difficult because of the turbulent nature of the laws of atmospheric motion. Their numerical integration is at a very high computational cost and often require empirical parameterizations. An alternative was suggested by Paltridge using a principle of Maximum Entropy Production.

In this work, we have developed a new formulation of Paltridge's model through a rigorous treatment of radiation. The resulting model is free of tunable coefficient, empirical parameterization and spurious assumption, therefore constituting a clean basis to evaluate the validity of the MEP hypothesis as applied to climate. In particular, we have been able to run a sensitivity experiment with respect to the surface albedo parameter corresponding to the presence of large ice-sheets in the Northern Hemisphere during the Last Glacial Maximum. The results for pre-industrial and LGM climates are found comparable with standard simulations with the IPSL_CM4 atmosphere-ocean general circulation model.

One of the strongest points in the model is certainly that it does not include any adjustable parameter. This ability to get rid of the usual, varyingly important, parameter calibration makes it a good candidate to investigate climates where little is known or where some phenomena are likely to be different from the usual parameterization validity range, like for instance climates of other planets, inside or outside the solar system, or paleoclimates.

Further developments also include coupling the model with a state-of-the-art radiative code to come up with a full three dimensional model, which would allow for more realistic paleoclimate simulations.

The basic idea of variational thermodynamic principles, such as the principle of Maximum Entropy Production, still remains to be proved. This study shows that it may however certainly be useful in application in the field of climate sciences, as well as in many others.⁸²

Present and Last Glacial Maximum climates as states of maximum entropy production:

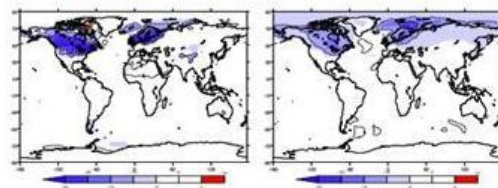


Figure 39 Surface temperature difference between Last Glacial Maximum conditions and present conditions at MEP states. **Right:** Surface temperature difference between Last Glacial Maximum conditions and present conditions for the IPSL model. The global mean LGM cooling is -2°C for the MEP model and -2.5°C for the IPSL model.

⁸²C. Herbert, D. Paillard, M. Kageyama, B. Dubrulle *Quart. J. Roy. Meteor. Soc.* **137** (2011) 1059-1069.

5.3.7 Boltzmann-Ginzburg-Landau approach to simple active matter models

Active matter loosely refers to all situations where some energy is spent locally to produce some directed, persistent motion. In this context, collective motion naturally occupies a central spot. The statistical physics approach has been, not surprisingly, aimed at uncovering generic, universal properties to be exhibited in many different situations. To this aim, simple “microscopic” (particle-, agent-based) models have been studied and continuous theories have been proposed.

Because the equations constituting these continuous “hydrodynamic” theories typically contain many terms, deriving them from generic, microscopic starting points is very important, since then all transport coefficients are defined in terms of a few microscopic control parameters, instead of having a huge parameter space with many “non-physical” regions. Previous attempts to get hydrodynamic equations for active matter suffer from the absence of control on the balance of the various terms. We have proposed to combine a classic kinetic theory approach with ideas from weakly nonlinear analysis, in order to obtain well-controlled, minimal, continuous field equations from simple models for collective motion.

Consider the celebrated Vicsek model where self-propelled particles move at constant speed v_0 , aligning their heading with local neighbors, with some noise. It has two key parameters, the global density of particles ρ_0 , and the noise strength σ . At low σ /large ρ_0 , a fluctuating, orientationally-ordered collectively moving phase exists, which typically presents spontaneously-segregated nonlinear structures and/or anomalous, long-range correlations.

In the dilute limit, where interactions are only binary, a Boltzmann equation rules the evolution of the one-particle function $f(r, \theta, t)$ representing the probability of finding a particle of orientation θ at time t and position r . To get hydrodynamic equations, one usually expands the above equation in Fourier series of the angular variable θ , yielding an infinite hierarchy of equations for various fields \hat{f}_k . While \hat{f}_0 is nothing but the density field, some \hat{f}_k actually represent “hydrodynamic fields” (\hat{f}_1 codes for a polarity field, \hat{f}_2 a tensorial field, etc.). For a problem where polar order emerges, one tries to write a closed equation for \hat{f}_1 , whose variations are assumed to be small and slow. Assuming, in this case, that \hat{f}_2, \hat{f}_3 , etc., are faster fields, one can express all these fields in terms of \hat{f}_1 . This formally yields an infinity of terms, and one then resorts to “counting gradients” to limit them.

Close enough to the transition at which order emerges, one can formalize, as in the Ginzburg-Landau approach to amplitude equations, an explic-

it scaling *ansatz* which allows to control all terms. We have applied this approach to the basic universality classes of self-propelled particles systems interacting solely by alignment. The obtained equations possess nonlinear solutions in excellent qualitative agreement with the behavior of the Vicsek-style models they are derived from. Some of these results are already published. This is yet another instance where the extra constraint of being near an instability actually helps to obtain well-behaved sets of equations observed to be valid well beyond this vicinity, as long as no other symmetry-breaking transition occurs.

For instance, in the case of “self-propelled rods” aligning nematically, the procedure described above yields, on top of the continuity equation, equations coupling the polar field f_1 and the tensorial field f_2 . A combination of analytical and numerical analysis of these coupled nonlinear partial differential equations shows that they are faithful, at a semi-quantitative level, to the original Vicsek-style model (see Figure 40).

All basic classes of “dry flocking” problems will soon have been treated using our approach.⁸³

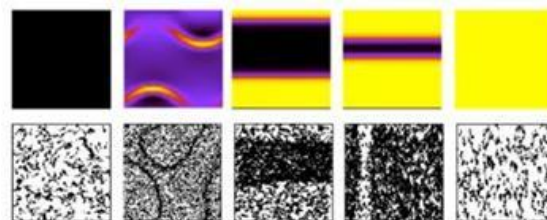


Figure 40 Snapshots of simulations of (i) the Vicsek model with nematic alignment (bottom row); (ii) the field equations derived using the Boltzmann-Ginzburg-Landau approach described here (top row) in two dimensions. For the microscopic model, a fraction of the particles are represented in each panel. For the continuous equations, the amplitude of the nematic field (f_2) is represented on a color scale going from black ($f_2=0$) to yellow (maximum value). In each case, 5 values of the noise strength σ are represented. From left to right, increasing σ : (i) homogeneous nematically-ordered state; (ii-iii) inhomogeneous ordered state with a nematic-like ordered dense band; (iv) space-time chaos of nematic bands; (v) homogeneous, microscopically-disordered state.

⁸³A. Peshkov, S. Ngo, E. Bertin, H. Chaté, F. Ginelli, *Phys. Rev. Lett.* **109** (2012) 098101; A. Peshkov, I. Aranson, E. Bertin, H. Chaté, and F. Ginelli, *Phys. Rev. Lett.* **109** (2012) 268701.

5.3.8 Emergence of collective motion in active and biological matter

The emergence of some order within an assembly of interacting objects is always fascinating to investigate. The observer is faced with many questions about the deep origin of this order and the precise conditions of its occurrence. By a statistical study of the collective motion of two-dimensional polymeric filaments moved by molecular motors, it was possible to retrieve the elementary interactions at the molecular level responsible for that organization. This result, published in the journal Nature, shows that in the case of biological objects, simple local interactions may be the cause of complex emerging phenomena.

The physics of active matter is a new topic dealing with systems where energy is spent locally to produce persistent, directed motion. Numerous situations are concerned in natural and in man-made systems at all scales, from the collective displacement of large groups of animals, swarms of robots without central control, bacteria and amoeba colonies, cells in organs, down to the subcellular level where molecular motors who transform chemical energy into mechanical work are in charge of many transport processes and of the general, large-scale integrity of the cell.

It is in this last context that well-controlled *in vitro* experiments on active matter are nowadays possible: purified biological components extracted from living cells are mixed in well-defined conditions, giving rise to large-scale, self-organized, cooperative phenomena which can be observed under the microscope via fluorescent marking.

The experiment performed in the group of Professor Kazuhiro Oiwa, at the Advanced Information and Communication Technology Research Institute near Kobe, Japan, consisted in putting microtubules (ubiquitous polymeric filaments present in most biological cells) in contact with a high-density carpet of dynein molecular motors⁸⁴ grafted to a substrate. In presence of ATP, the dynein heads attach to the microtubules and cooperatively move them around in a smooth, steady, two-dimensional motion. In a few minutes, a lattice of vortices spontaneously appear, which have a very large diameter (about 400 μm) compared to the microtubule's length (about 10 μm).

Under the supervision of Hugues Chaté, the analysis of further experiments performed on isolated filaments and the construction of a semi-quantitative mathematical model have allowed to show that only two basic ingredients are at the origin of the organized collective motion of millions of filaments forming the vortex lattice: the smooth, reptation-like motion of isolated microtu-

bules and their physical collisions leading to nematic alignment.

This set of results⁸⁵ constitutes a breakthrough in the field since it has allowed to show clearly on a real case what often remains a belief, albeit a well-grounded one, in theoretical statistical physics: a minimal set of simple mechanisms is sufficient to account quantitatively for complex emergent phenomena. Beyond this intellectual satisfaction, these results have also an important potential relevance in biology, in particular for understanding the formation of the plant cell cortex. More generally, they could be exploited in the quest for novel biomaterials.

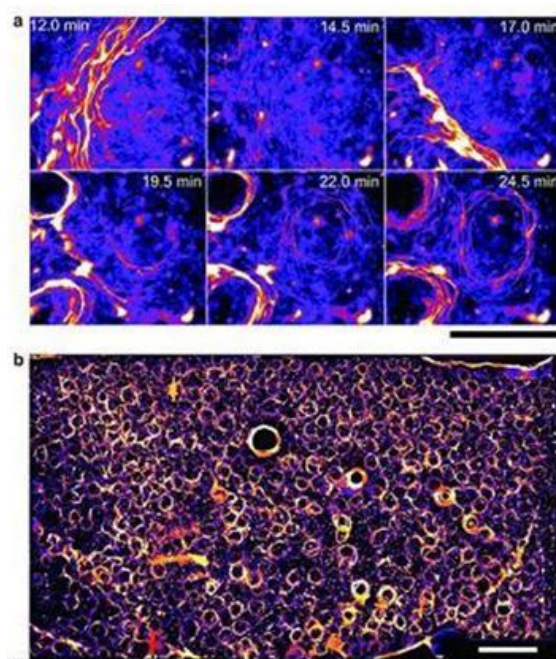


Figure 41 (a) Vortex formation. Scale: 500 μm , equivalent to approximately 40 times the microtubule length. (b) Typical image of the system after 30 minutes. Scale: 2 mm.

⁸⁴Dyneins: protein complexes of about 2 M Dalton, comprising two heavy chains, seven or eight intermediate chains and two light chains. The dyneins are active in association with a protein complex: the dyneactin, motor protein in animal cells.

⁸⁵Y. Sumino, K.H. Nagai, Y. Shitaka, D. Tanaka, K. Yoshikawa, H. Chaté and K. Oiwa, *Nature*, **483** (2012) 448.

5.3.9 Folding transition in a synthetic peptide: evidence of a three state non-cooperative process.

New precise measurements of circular dichroism in poly(L-glutamic) acid put into question the long admitted theory of the coil helix transition in this molecule and provide evidence a quite different mechanism.

Proteins are essential building blocks of life. They exhibit multiple properties due to the interplay between their four structural levels: primary (aminoacids sequence), secondary (alpha helices, beta sheets, etc.), tertiary (arrangements of secondary structures in space) and quaternary (self-assembly of supramolecular structures). The primary structure is fixed by covalent bonds and is therefore very stable. The other levels of order are governed by much weaker interactions (hydrogen bonds, dipolar interactions, etc.) and are therefore sensitive to changes in the environment such as temperature, pH, etc. Understanding the formation of these structures is an important step in the understanding of their overall properties. Moreover it is strongly suspected that the misfolding of some proteins is responsible for serious diseases such as prion-related diseases or Alzheimer's disease.

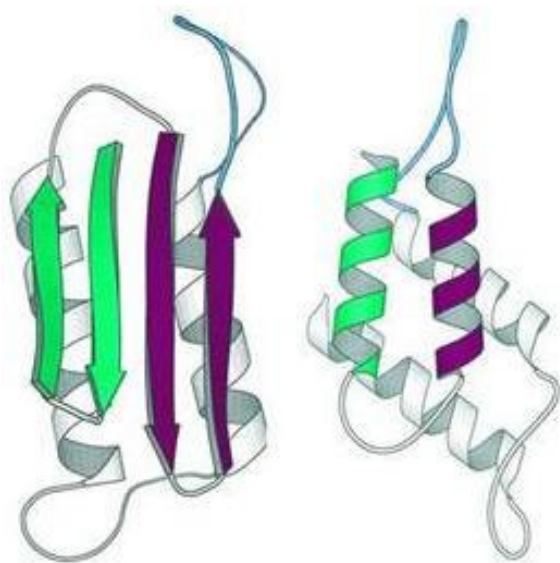


Figure 42 Two folding states of the prion molecule. Green and purple parts can be in beta sheet (left, an arrow schematizes a beta sheet) or alpha helix (right) configuration.

Among all the possible polyaminoacids, the one containing only glutamic side groups - poly(L-glutamic) acid or PGA - was usually considered as folding only as alpha helix while others can present several structures in equilibrium. It was therefore a good choice for elaborating and testing static models of the alpha helix thermodynamic parameters or dynamic models of the folding kinetics (after a laser induced temperature jump for instance) The amount of helices can be directly measured using circular dichroism and a set of measurements at different

concentrations spanning the largest possible temperature range has been performed using a state-of-the-art JASCO J-815 CD spectrometer.⁸⁶

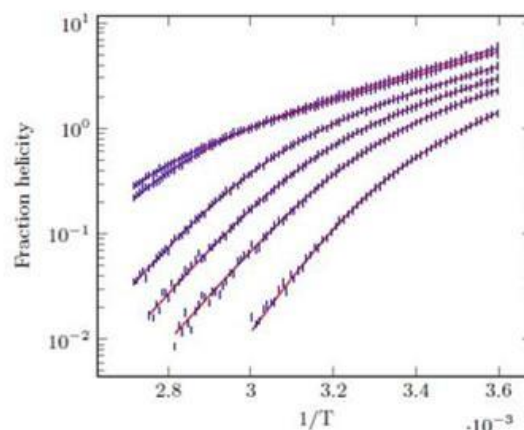


Figure 43 Fraction of helices vs. reciprocal temperature. Data points are vertical bars and the red line is the best fit by a three state non-cooperative model.

Up to now, a theory developed in 1959 by Zimm and Bragg⁸⁷ was considered as adequate for the description of the transition of PGA between the helix state and the random coil one. This theory is very similar to the 1D Ising model. A “spin” is a helical configuration of a part of the chain and the main feature is a coupling energy that favors the “alignment” of contiguous “spins”. In the coordinates of Figure 43, this would be represented by a sigmoidal (“S”) shape, the increase of the slope in the middle region being directly related to the coupling energy. The experimental results clearly do not fit with such a shape.

Indeed the shape of each data set can be more accurately described as two linear parts matched by a smooth crossover which hints that the transition involves two different equilibria involving therefore three states of the molecule. Only one of these states is optically active (the helix one). The newly introduced state is not active and is very probably of beta sheet type. A fit assuming these three states and no coupling constant is very satisfactory.⁸⁸

⁸⁶A. Koutsioubas, D. Lairez, S. Combet, G. Fadda, S. Longeville and G. Zalczner, *J. Chem. Phys.* **136** (2012) 215101.

⁸⁷B. H. Zimm and J. K. Bragg, *J. Chem. Phys.* **31** (1959) 526.

⁸⁸G. Zalczner *Eur. Phys. J.* **E35** (2012) 100.

5.3.10 Huge Seebeck coefficients of macro-ions in organic electrolytes

(see also GMT, page 54)

The shortage in fossil fuel resources has encouraged a huge effort towards the research of alternative sustainable energy. Within this framework, thermoelectricity offers the possibility to convert low-grade waste heat (including solar heating) into electric power. When a temperature gradient ΔT is applied to an isolated conducting rod, the electrons at the hot part acquire some kinetic energy and diffuse to the cold part, resulting in the creation of an electric field $E = -\Delta V = S\Delta T$. The proportionality coefficient S is called “Seebeck coefficient”, from the name of the German physicist who discovered this effect. A tremendous effort is currently accomplished in the field of solid-state thermoelectric devices (more than 9,000 publications during the last decade). However, the research of new solid-state thermoelectric materials has reached its limits and most efforts are now devoted to the increase of the conversion efficiency through nanostructuring, which incurs a substantial manufacturing cost.

The alternative possibility—to use electrolytes instead of electron or holes as charged carriers—to convert a temperature gradient into an electromotive force is still underexplored. With electrons or holes as carriers the Seebeck coefficient in solid-state thermoelectric devices is only of a few hundreds of $\mu\text{V}/\text{K}$. But since it is proportional to the entropy carried by the moving charges, it could reach much higher values in electrolytes containing macro-ions.

We have recently observed huge Seebeck coefficients up to 7 mV/K for tetra-alkyl-ammonium ions in alkanes⁸⁹ (cf. Figure 44).

The fluid sample is contained in a 14 mm high and 14 mm diameter cylindrical Teflon cell, with both ends closed by sapphire windows. The cell is positioned vertically and heated from the top by a thin film resistance. The lower window is maintained at a constant temperature. Two platinum or carbon-glass electrodes are inserted in electrically insulating tubes and positioned horizontally with their exposed flat tips (~ 1 mm in diameter) placed 6 mm apart along the vertical axis. The temperature gradient along this axis is verified to be stable. The open circuit voltage ΔV between the two electrodes is measured via a high impedance electrometer.

These unprecedented S values are unfortunately compensated by a poor electrical conductivity which lowers the figure of merit. We are now focusing on binary mixtures of ionic-liquid/organic solvent whose ionic conductivities are closer to the electronic conductivities achieved in solid-state thermoelectric devices. Such binary mixtures are now widely used in lithium batteries and supercapacitors. After adding a redox couple which allows a reversible exchange of electrons between the liquid and the electrodes, we have observed a strong

enhancement of the associated Seebeck coefficient at high ionic-liquid concentrations.⁹⁰

This research program has been initiated owing to the support of the DSM-ENERGY program “FLUIDES ThermoElectriques” and is continuing through ANR Progelec Program “ThermoElectric Ferrofluids, Ionic Liquids and Colloids” (TEFLIC), in collaboration with PECSA laboratory at UPMC. This project includes the study of:

- Charging of Li cells or supercapacitors through a temperature gradient, using ionic-liquids/organic-solvent binary mixtures and electrodes coated with active carbon.
- The combined thermoelectric and magnetothermic effects in charged ferrofluids.
- The enhancement of the Seebeck effect due to entropy change at the phase transition in thermo-sensitive colloidal suspensions.

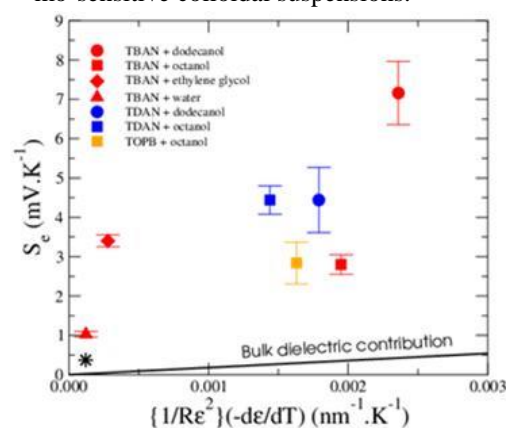


Figure 44 Seebeck coefficients of various tetra-alkyl-ammonium ions in alkanes. The straight line represents a bare electrostatic contribution proportional to $d(1/4\pi\epsilon R)/dT$, where ϵ is the dielectric constant and R the effective radius of ions. The much higher measured values are due to entropic effects related to the interaction of ions with the solvent.

⁸⁹M. Bonetti, S. Nakamae, M. Roger and P. Guenoun, *J. Chem. Phys.* **134** (2011) 114513.

⁹⁰V. Zinovyeva, S. Nakamae, M. Bonetti, M. Roger., *ChemElectroChem* (2013) DOI:10.1002/celec.201300074.